

# Bed-limited cracks in effective medium theory

S. R. Tod<sup>1,2,\*</sup>

<sup>1</sup>Department of Applied Mathematics and Theoretical Physics, University of Cambridge, Silver Street, Cambridge CB3 9EW, UK.

E-mail: S.R.Tod@damtp.cam.ac.uk

<sup>2</sup>British Geological Survey, West Mains Road, Edinburgh EH9 3LA, UK

Accepted 2002 August 6. Received 2002 July 22; in original form 2002 January 18

## SUMMARY

An effective medium theory typically requires the description of a mean crack shape. In general, for simplicity, this is taken to be a flat, circular ('penny-shaped') crack. However, this places an unnecessary limitation on the theory, when it is perhaps more realistic to describe a crack in terms of having a bounded width and an otherwise ellipsoidal shape. The generalization of the method of smoothing, as proposed by Hudson (1994, *Geophys. J. Int.*, **117**, 555–561), to extend his original model (Hudson, 1980, *Math. proc. Camb. phil. Soc.*, **88**, 371–384), has been used to study the role of the crack width and the ratio of the two larger dimensions in determining the properties of the effective medium. In general, this leads to a description of the medium as having orthorhombic symmetry, and provides a suitable description of a material where the crack dimensions are restricted in one direction owing to, for example, bed-limiting effects, while remaining unconfined in other directions. An elliptical flat crack limit is determined, analogous to the circular crack description of the original Hudson model. In addition to the isolated crack description, the theory is extended to include the fluid flow mechanism of Tod (2001, *Geophys. J. Int.*, **146**, 249–263) that models the flow as being dominated by crack-to-crack flow and is valid for low matrix porosities and over a large range of frequencies, provided that the wavelength is much greater than the crack dimensions.

**Key words:** anisotropy, cracked media, porosity.

## 1 INTRODUCTION

Effective medium theories have been developed that give the overall properties of an elastic material containing cracks by a number of authors (e.g. Hudson 1980; O'Connell & Budiansky 1974; Nishizawa 1982). While these methods have been developed using a range of different techniques, they all require the calculation of the response of a single crack. In general, this is calculated in the limit in which the thickness of the crack vanishes (Garbin & Knopoff 1973; Hudson 1980; O'Connell & Budiansky 1974; Walsh 1965) and the cracks are assumed to be either dry (Garbin & Knopoff 1973; Hudson 1981; O'Connell & Budiansky 1974; Walsh 1965) or fluid-filled (Anderson *et al.* 1974; Garbin & Knopoff 1975; Hudson 1981; O'Connell & Budiansky 1977). While these cracks are often circular ('penny-shaped') they may also be elliptical (Bai *et al.* 2000; Budiansky & O'Connell 1976; Tsukrov 2000; Tsukrov & Kachanov 2000). Ellipsoids of a non-zero thickness give rise to more general formulations (Eshelby 1957; Hudson 1994; Kuster & Toksöz 1974; Nishizawa 1982; Sayers 1988) and more general crack shapes have also been studied in the 2-D problem (Mavko & Nur 1978; Walsh & Grosenbaugh 1979; Tsukrov & Novak 2002).

While these models consider a range of crack shapes, orientations and material infill, they assume the cracks to be isolated, without fluid connections. The mechanism that dominates the fluid flow process depends upon the relative scale of the crack network and the pore structure in which it is embedded, and which provides the mechanism for allowing fluid to flow within the material. The fluid flow may be controlled by a crack-to-crack flow (Hudson *et al.* 1996; Tod 2001), diffusion into the matrix material, equant porosity (Hudson *et al.* 1996; Thomsen 1995), or by a squirt flow mechanism from one region of a crack to another (Chapman 2001; Mavko & Jizba 1991). Alternatively, the movement of fluid within a matrix rock may occur entirely within the porosity of the matrix rather than being influenced by the network of cracks (e.g. Gassmann 1951; Biot 1956) or may be a balance between the porosity of the pore space and that of the crack network (Auriault & Boutin 1994).

Most effective medium theories predict that the overall properties of a cracked medium are frequency independent when, in fact, a frequency dependence may arise as a result of a number of alternative mechanisms; including fine elastic layering (Shapiro & Hubral 1996), scattering at shorter wavelengths (Chesnokov *et al.* 2001) or a fluid flow mechanism (Chapman 2001; Hudson *et al.* 1996; Tod 2001).

Experimental work at ultrasonic ( $1 \times 10^6$  Hz) and logging ( $1 \times 10^4$  Hz) frequencies and observations at seismic (10–100 Hz)

\*Now at: Bp Exploration, Chertsey Road, Sunbureyon Thames, Middlesex, TW16 7LN, UK. E-mail: tods01@bp.com.

frequencies suggest that, in fact, the material properties of a cracked solid display a frequency dependence in the presence of fluid (Rathore *et al.* 1995; Sothcott *et al.* 2000; Spencer 1981; Winkler 1985), are sensitive to crack aspect ratio (Rathore *et al.* 1995) and to crack size (Borgos *et al.* 2000; Lore *et al.* 2001; Roy *et al.* 2001).

It is these considerations, then, that lead us to develop a model that combines previous work on cracks of arbitrary ellipsoidal shape in an elastic matrix and fluid flow between cracks that leads to a description of the effective properties of the medium that is frequency dependent, as a direct result of the fluid flow mechanism. The theory is valid over a large frequency range provided that the wavenumber remain less than the crack length and is appropriate for matrix rock of low porosity. The application of the theory to modelling exploration and earthquake data has been undertaken in a separate study (Tod & Liu 2002).

**2 THE INCLUSION PROBLEM**

The method of smoothing (Keller 1964), used by Hudson (1980) to derive an effective medium theory for aligned circular cracks embedded within an isotropic background matrix, was extended by Hudson (1994) to include aligned identical cavities or inclusions described by spheroids of non-zero thickness.

Defining the elastodynamic operator  $\mathcal{L}$  such that

$$\mathcal{L}_{ip}u_p = \left( \frac{\partial}{\partial x_j} c_{ijpq}^0 \frac{\partial}{\partial x_q} + \rho_0 \omega^2 \delta_{ip} \right) u_p, \tag{1}$$

where  $c^0$  are the elastic stiffnesses of the isotropic matrix material and  $\rho_0$  its density, Hudson (1980) derives the equation for the mean field  $\langle \mathbf{u} \rangle$  as

$$\left[ \mathcal{L}_{ip} - \epsilon v^s \int_{\mathcal{D}} dV_x \mathcal{L}_{ij} \bar{S}_{jp}(\mathbf{x}) + \mathcal{O}(\epsilon^2) \right] \langle u_p \rangle = 0, \tag{2}$$

where  $v^s$  is the number density of cracks,  $\epsilon \bar{S}(\mathbf{u})$  is the scattered wavefield generated by an averaged crack from an incident field  $\langle \mathbf{u} \rangle$ ; the small parameter  $\epsilon$  indicates that the scattered field is small in comparison with the incident wave, and integration is over the entire medium. The summation convention is assumed throughout. Neglecting terms of order  $\epsilon^2$  and above ignores crack–crack scattering.

We approximate the mean wave by a plane wave

$$\langle \mathbf{u} \rangle = \mathbf{b} e^{i\mathbf{k}\cdot\mathbf{x}}, \tag{3}$$

so that

$$\mathcal{L}_{ip} \langle u_p \rangle = (\rho_0 \omega^2 \delta_{ip} - c_{ijpq}^0 k_j k_q) b_p e^{i\mathbf{k}\cdot\mathbf{x}}. \tag{4}$$

Use of the reciprocity theorem yields an expression for the scattered wave (Hudson 1994; Kuster & Toksöz 1974)

$$\epsilon \bar{S}_{jp} \langle u_p \rangle(\mathbf{x}) = \int_V \left[ \rho^+ \omega^2 G_{jp}(\mathbf{x}, \mathbf{y}) - c_{ikpq}^+ \frac{\partial G_{ji}(\mathbf{x}, \mathbf{y})}{\partial y_k} \frac{\partial}{\partial y_q} \right] u_p(\mathbf{y}) dV_y, \tag{5}$$

where

$$\mathbf{u} = \langle \mathbf{u} \rangle + \mathbf{u}' \tag{6}$$

is the wavefield inside the inclusion or cavity,  $\mathbf{G}(\mathbf{x}, \mathbf{y})$  is the Green function satisfying

$$\mathcal{L}_{ip} G_{pj}(\mathbf{x}, \mathbf{y}) = -\delta_{ij} \delta(\mathbf{x} - \mathbf{y}) \tag{7}$$

and  $\rho^+$  and  $c^+$  are defined as

$$\rho^+ = \rho' - \rho_0 \tag{8}$$

and

$$c^+ = c' - c^0, \tag{9}$$

where  $\rho'$  and  $c'$  are the density and elastic stiffnesses of the inclusion, respectively. A certain amount of care is required (Hudson 1994) in the case of a cavity, as there is no actual displacement within  $V$ . Essentially, we may still use eq. (5), on the understanding that there is an artificial displacement within the cavity.

In the low-frequency (static) approximation, the total displacement  $\mathbf{u}$  and strain  $\mathbf{e}$  within the inclusion are given by Hudson (1994) as

$$\mathbf{u}(\mathbf{x}) = \langle \mathbf{u} \rangle(\boldsymbol{\xi}) + V'(\mathbf{x} - \boldsymbol{\xi})\langle \mathbf{e} \rangle(\boldsymbol{\xi}) \tag{10}$$

and

$$\mathbf{e}(\mathbf{x}) = \langle \mathbf{e} \rangle(\boldsymbol{\xi}) + E'(\mathbf{x} - \boldsymbol{\xi})\langle \mathbf{e} \rangle(\boldsymbol{\xi}) = E(\mathbf{x} - \boldsymbol{\xi})\langle \mathbf{e} \rangle(\boldsymbol{\xi}), \tag{11}$$

defining  $E$ , where  $V'$  and  $E'$  are perturbations to the mean wave state and  $\boldsymbol{\xi}$  is the centroid of  $V$ . Hudson (1994) neglects the second term of eq. (10) on the physical grounds that it is of lower order than the first term, as seen in studies of diffraction by a sphere (Ying & Truell 1956), and defines  $E$  for an ellipsoidal inclusion with lengths  $2a$ ,  $2b$  and  $2c$  along the  $x_1$ ,  $x_2$  and  $x_3$  axes respectively, as

$$E = (\mathcal{S} s^0 c^+ + \mathbf{I})^{-1}, \tag{12}$$

in terms of the Eshelby tensor  $\mathcal{S}$  (Eshelby 1957), with

$$a \geq b \geq c, \tag{13}$$

$s^0$  the compliance tensor of the isotropic matrix material, and the identity tensor

$$I_{ijkl} = \frac{1}{2}(\delta_{ik}\delta_{jl} + \delta_{il}\delta_{jk}). \tag{14}$$

Inserting eq. (5) into eq. (2) and using eqs (10), (11) and (3),

$$(\rho \omega^2 \delta_{ip} - c_{ijpq} k_j k_q) b_p = 0, \tag{15}$$

where the density and elastic stiffnesses are given by

$$\rho = \rho_0(1 - s) + \rho' s \tag{16}$$

and

$$c = c^0 + c^1, \tag{17}$$

where

$$c^1 = s c^+ E \tag{18}$$

and

$$s = \frac{4}{3} \pi v^s abc \tag{19}$$

is the volume density of inclusions, the ratio of the volume occupied by the cracks to the total volume, so it may be identified with the porosity of the medium.

For a range of crack orientations and dimensions, an additional averaging process is required. This can be effected by summing over sets of cracks with identical orientation and dimension.

3 THE THIN-CRACK LIMIT

Let us assume that the lengths  $a, b$  and  $c$  obey

$$a \geq b \gg c \tag{20}$$

and look at the limit in which

$$\alpha = c/a \rightarrow 0. \tag{21}$$

Clearly, from eq. (19)

$$s \rightarrow 0 \tag{22}$$

thus from eq. (16)

$$\rho \rightarrow \rho_0. \tag{23}$$

However, the asymptotic behaviour of eq. (18) requires determination of the limit of  $\alpha E$ . This requires inverting the tensor

$$A = Ss^0 c^+ + I \tag{24}$$

where the components of  $A$  are given by

$$A_{ijkl} = \frac{1}{3} \left( \frac{\kappa'}{\kappa} - \frac{\mu'}{\mu} \right) S_{ijpp} \delta_{kl} + \left( \frac{\mu'}{\mu} - 1 \right) S_{ijkl} + I_{ijkl}, \tag{25}$$

where  $\nu$  is Poisson's ratio for the matrix material,  $\kappa, \mu$  are its bulk and shear moduli, and  $\kappa'$  and  $\mu'$  are the bulk and shear moduli of the inclusion.  $S$  and hence  $A$  has the symmetries

$$S_{ijkl} = S_{ijlk} = S_{jikl}. \tag{26}$$

If we write

$$A = A^0 + \alpha A^1 + O(\alpha^2) \tag{27}$$

then clearly we require  $A^0$  to be singular for the limit of  $\alpha E$  as  $\alpha \rightarrow 0$  to be non-zero. The components of  $A^0$  are given by eqs (A1)–(A5). Unless  $\mu' = 0$ ,  $A^0$  is invertible and  $c^1 \rightarrow 0$ . If  $\mu' = 0$  we require components of  $A^1$  (eqs A6–A10) to determine  $\alpha E$  (eqs A11–A14).

3.1 Dry and fluid-filled cracks

If  $\kappa' = 0$  in addition to  $\mu' = 0$ , then

$$c_{ijkl}^1 = -\frac{\epsilon}{\mu} c_{p3ij}^0 c_{q3kl}^0 U_{pq}, \tag{28}$$

as the result of Hudson (1980), where  $U$  is a diagonal tensor with elements

$$U_{11} = \frac{8}{3} \frac{1 - \nu}{1 + \nu[f(b/a) - 1]} \tag{29}$$

$$U_{22} = \frac{8}{3} \frac{1 - \nu}{1 - \nu f(b/a)} \tag{30}$$

and

$$U_{33} = \frac{8}{3} (1 - \nu). \tag{31}$$

The function  $f$  is defined as

$$f(z) = z^2 D/E \tag{32}$$

and the crack density is given by

$$\epsilon = \nu^s \frac{2A^2}{\pi P}, \tag{33}$$

as Budiansky & O'Connell (1976), where  $A = \pi ab$  is the area of the crack,  $P = 4aE$  is the perimeter and, following the notation of Gradshteyn & Ryzhik (1980),

$$E \equiv E(\pi/2, y), \tag{34}$$

$$D \equiv D(\pi/2, y) = [F(\pi/2, y) - E(\pi/2, y)]/y^2, \tag{35}$$

where

$$y^2 = 1 - z^2 \tag{36}$$

and  $F(\theta, y)$  and  $E(\theta, y)$  are elliptic integrals of the first and second kind, respectively.

In the further limit in which

$$b/a \rightarrow 1, \tag{37}$$

we have that

$$D/E \rightarrow \frac{1}{2} \tag{38}$$

and  $U_{11}, U_{22}$  and  $\epsilon$  reduce to the original expressions of Hudson (1981);

$$U_{11} = U_{22} = \frac{16}{3} \frac{1 - \nu}{2 - \nu} \tag{39}$$

and

$$\epsilon = \nu^s a^3. \tag{40}$$

The fluid-filled case, in which  $\kappa' \neq 0$ , leads to the same form for  $c^1$ , but with  $U_{33} = 0$ , as given by Hudson (1981).

3.2 Cracks filled with weak material

Finally, we may look at the case where  $\mu' \neq 0$  and  $\kappa' \neq 0$  for small (non-zero) values of  $\mu'/\mu, \kappa'/\kappa$  and  $\alpha$ , keeping only terms of order  $\alpha\mu/\mu'$  and  $\alpha\kappa/\kappa'$ , so that there is a large contrast between the parameters of the inclusion and those of the matrix. The non-zero components of  $\alpha E$  are given by eqs (A15)–(A18) and we may write the first-order correction to the elastic constants in the form of eq. (28) with the crack density being given by eq. (33),

$$U_{11} = \frac{8}{3} \frac{1 - \nu}{1 + \nu[f(b/a) - 1]} (1 + M_1)^{-1}, \tag{41}$$

$$U_{22} = \frac{8}{3} \frac{1 - \nu}{1 - \nu f(b/a)} (1 + M_2)^{-1} \tag{42}$$

and

$$U_{33} = \frac{8}{3} (1 - \nu)(1 + K)^{-1}, \tag{43}$$

with

$$M_1 = \frac{b}{\alpha\alpha E} \frac{1 - \nu}{1 + \nu[f(b/a) - 1]} \frac{\mu'}{\mu}, \tag{44}$$

$$M_2 = \frac{b}{\alpha\alpha E} \frac{1 - \nu}{1 - \nu f(b/a)} \frac{\mu'}{\mu} \tag{45}$$

and

$$K = \frac{b}{\alpha\alpha E} (1 - \nu) \left( \frac{\kappa'}{\mu} + \frac{4}{3} \frac{\mu'}{\mu} \right). \tag{46}$$

This agrees with the result given by Hudson (1981) in the case when  $a = b$ .

### 4 RESULTS FOR VARYING CRACK DIMENSIONS

The wave speeds  $v_i, i = 1, 2, 3$ , of the resulting anisotropic material may be found by solving the dispersion equation

$$\det(\rho v^2 \delta_{ip} - c_{ijpq} \hat{k}_j \hat{k}_q) = 0, \tag{47}$$

where  $\hat{\mathbf{k}} = \mathbf{k}/k$  is the normalized wavenumber vector.

Let us first look at the case in which the dimensions  $a, b$  and  $c$  of the bed-limited cracks are fixed and the width of the crack  $c$  is non-zero. The resulting effective medium exhibits orthorhombic anisotropy. Figs 1(a) and (b) display the variation in wave speeds with offset angle  $\theta$ , where the azimuthal angle  $\phi = 0^\circ$  is fixed. In Figs 1(c) and (d) the azimuthal angle  $\phi$  varies, with  $\theta = 30^\circ$  fixed. In all, the fixed ratios  $b/a = \frac{1}{3}$  and  $c/a = \frac{1}{300}$  are used, with  $b = 1$  m and  $v^s = 0.01 \text{ m}^{-3}$ , so that the porosity  $s = 1.3 \times 10^{-3}$ .  $\theta$  is defined to be the angle between the incident wave and the vertical axis, whereas  $\phi$  is the angle from the axis in the horizontal plane lying parallel to the direction of minimum crack width. Fig. 2 demonstrates the effect on the wave speeds caused by letting the ratio  $c/a \rightarrow 0$ , while keeping  $b/a$  and  $v^s$  fixed at the values used in Fig. 1, and  $\theta = 30^\circ$  and  $\phi = 30^\circ$  fixed. This corresponds to letting the crack width  $c \rightarrow 0$ , reducing the porosity likewise, so that the limiting values corresponding to eq. (28) are reached. In Fig. 3 the crack length  $a \rightarrow \infty$  by allowing the ratio  $b/a \rightarrow 0$  while keeping  $b/c$  and  $s$  fixed. It does not make sense in this case to keep the crack density  $v^s$  fixed, as this will result in a porosity greater than unity at a finite crack length. The limiting values at  $b/a = 0$  corresponds to an infinite cylinder, in other words a 2-D result. Throughout, the matrix is taken to have material properties  $v_p = 3.5 \times 10^3 \text{ m s}^{-1}$ ,  $v_s = 2.0 \times 10^3 \text{ m s}^{-1}$ , the compressional and shear wave speeds of the uncracked matrix, and  $\rho = 2.2 \times 10^3 \text{ kg m}^{-3}$ , while the cracks are assumed to be filled with water.

From Figs 1(a) and (b) we see that the compressional wave speed and one of the shear wave speeds varies as  $2\theta$ , while the second shear wave speed varies as  $4\theta$ , such that there are two angles at which the shear wave splitting vanishes. A significant change in wave speeds with offset is seen, for even a modest value of the porosity. An increase in  $s$  will result in an increase in the anisotropy. Figs 1(c) and (d) indicate a similarly large range of variation in the wave speeds with azimuth at a fixed offset. This will hold for all but the zero-offset measurement. The three wave speeds vary as  $2\phi$  and we notice, in particular from the two shear wave speeds, that the level of shear wave splitting varies substantially with azimuth.

Figs 2(a) and (b) exhibit a roughly linear dependence of wave speeds with crack thickness, while Figs 3(a) and (b) show an approximately linear variation in the wave speeds with crack length. The trend in Fig. 2 is as expected, for the crack width increase, so does the volume density of cracks (the porosity), therefore the greater the weakening in the material is, the lower the material stiffnesses. In Fig. 3 we see that as the volume of the average crack increases, i.e.  $b/a \rightarrow 0$ , the wavespeeds decrease and the shear wave splitting increases.

### 5 ADDING FLUID FLOW

If we assume that the cracks are not all aligned and not all identical in size, we may write

$$c_{ijkl}^1 = \sum_n s^n c_{ijpq}^+ E_{pqkl}^n, \tag{48}$$

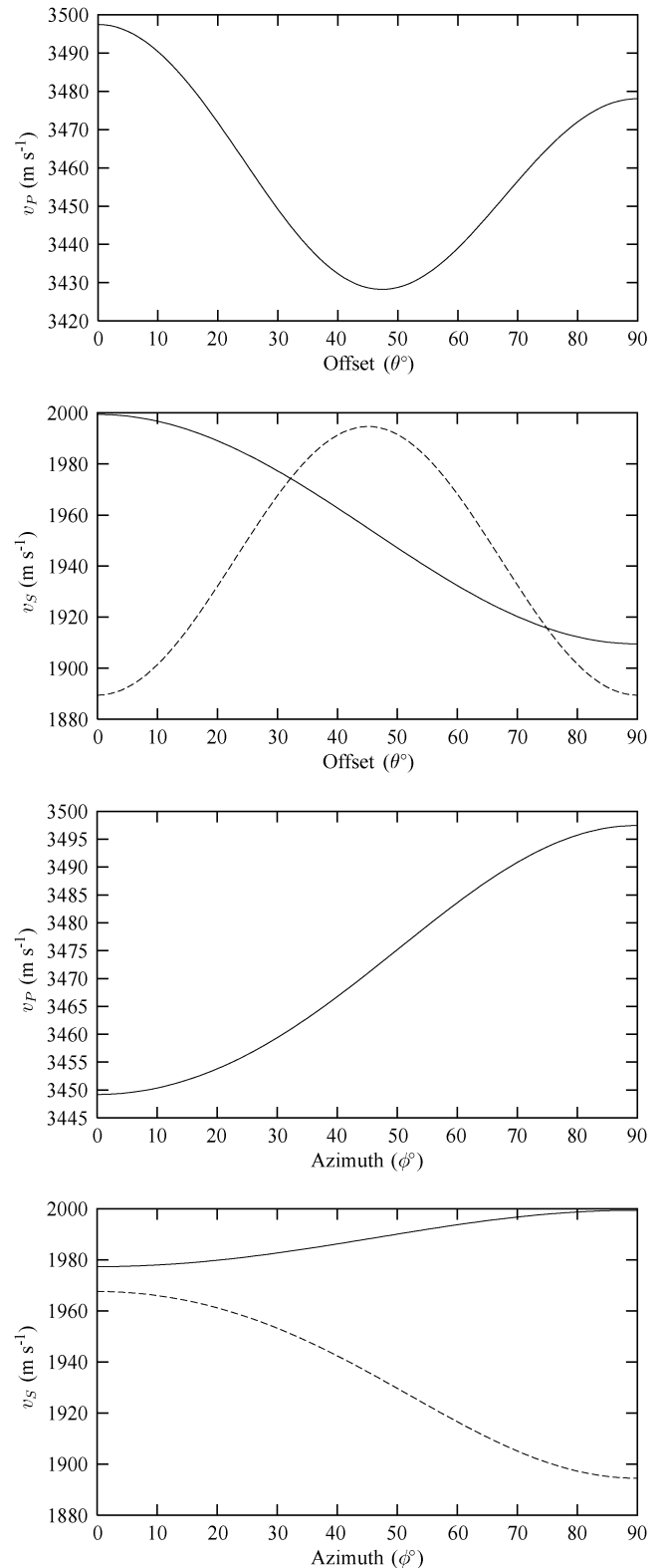


**Figure 1.** (a) The variation in compressional wave speed with offset at an azimuth parallel to the smallest crack dimension. (b) As in (a), but for shear wave speeds. The solid line corresponds to the quasi-SV wave and the dashed line to the quasi-SH wave. (c) The variation in compressional wave speed with azimuth at an offset of  $30^\circ$ . (d) As in (c), but for shear wave speeds. The solid line corresponds to the quasi-SV wave and the dashed line to the quasi-SH wave.

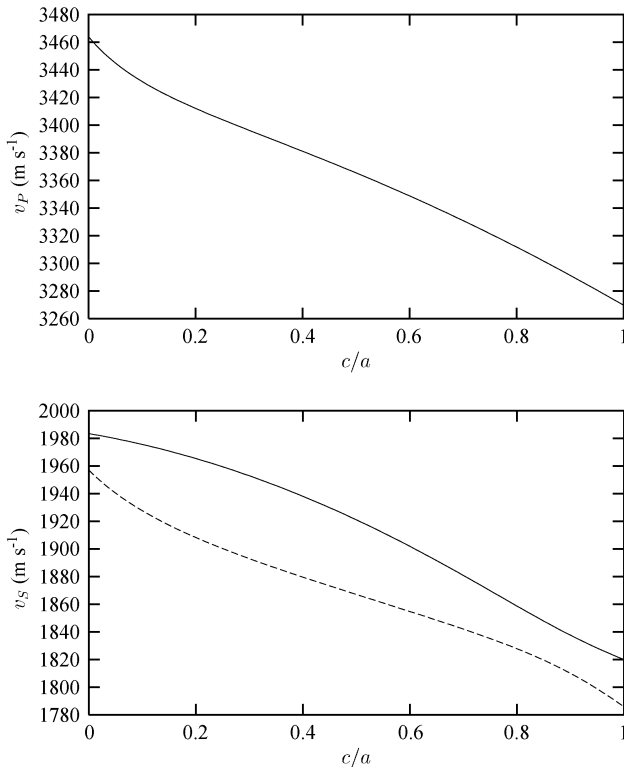


**Figure 2.** (a) The variation in compressional wave speed with the ratio of the crack width to length for a fixed crack density at an offset of 30° and an azimuth of 30°. (b) As in (a), but for shear wavespeeds. The solid line corresponds to the quasi-SV wave and the dashed line to the quasi-SH wave.

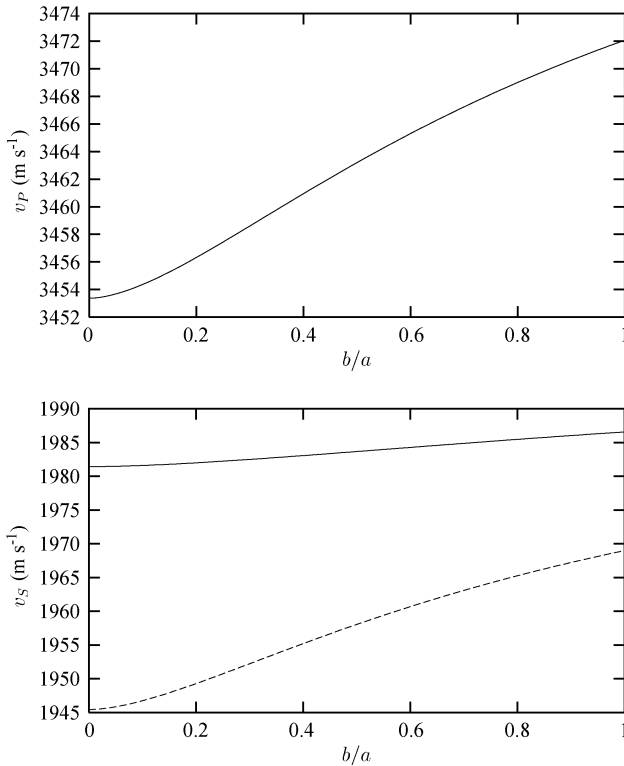


**Figure 3.** (a) The variation in compressional wave speed with the ratio of the crack height to length for a fixed porosity at an offset of 30° and an azimuth of 30°. (b) As in (a), but for shear wave speeds. The solid line corresponds to the quasi-SV wave and the dashed line to the quasi-SH wave.

where

$$E_{pqkl}^n = E_{mnrsl} \ell_{mp}^n \ell_{nq}^n \ell_{rk}^n \ell_{sl}^n, \quad (49)$$

the superscript  $n$  labels the cracks, and  $\ell^n$  rotates from the background (global) axes to (local) axes fixed in the  $n$ th crack with the  $x_1, x_2$  and  $x_3$  axes along the directions with lengths  $2a, 2b$  and  $2c$ .  $\ell^n$  is given in terms of the Euler angles  $\theta, \phi$  and  $\psi$  by

$$\ell^n = \begin{pmatrix} \cos \theta \cos \phi \cos \psi & \cos \theta \sin \phi \cos \psi & -\sin \theta \cos \psi \\ -\sin \phi \sin \psi & +\cos \phi \sin \psi & \\ -\cos \theta \cos \phi \sin \psi & -\cos \theta \sin \phi \sin \psi & \sin \theta \sin \psi \\ -\sin \phi \cos \psi & +\cos \phi \cos \psi & \\ \sin \theta \cos \phi & \sin \theta \sin \phi & \cos \theta \end{pmatrix}, \quad (50)$$

and if  $\mathbf{e}_1, \mathbf{e}_2$  and  $\mathbf{e}_3$  form a right-handed triad of unit vectors that describe the orientation of an ellipsoidal inclusion in the global axes, then

$$\ell_n = (\mathbf{e}_1 \mathbf{e}_2 \mathbf{e}_3)^T. \quad (51)$$

The strain  $\mathbf{e}^n$  in inclusion  $n$  as a result of an imposed strain  $\mathbf{e}^0$  at infinity is given by

$$\mathbf{e}^n = \mathbf{E}^n \mathbf{e}^0. \quad (52)$$

To determine the strain  $\mathbf{e}^n$  owing to an imposed stress  $\boldsymbol{\sigma}^0$  at infinity and a pressure  $p^n$  within the crack we subtract a uniform field  $\boldsymbol{\sigma} = -p^n \mathbf{I}$  from the stress field in the matrix leaving a structure with imposed stress  $\boldsymbol{\sigma}^0 + p^n \mathbf{I}$  at infinity. The strain caused by the superposition of these two fields is

$$e_{ij}^n = \bar{E}_{ijkl}^n s_{klpq}^0 (\sigma_{pq}^0 + p^n \delta_{pq}) - \frac{p^n}{3\kappa} \delta_{ij}, \quad (53)$$

where  $\kappa = \lambda + 2\mu/3$  is the bulk modulus of the matrix and  $\bar{E}^n$  is related to  $\bar{E}$  by eq. (49), where

$$\bar{E} = (\mathbf{I} - \mathbf{S})^{-1}, \quad (54)$$

the dry result of eq. (12).

To relate the pressure in the  $n$ th crack  $p^n$  to the imposed stress  $\boldsymbol{\sigma}^0$  we use the fluid flow model of Hudson *et al.* (1996) and Tod (2001) where the porosity in the  $n$ th crack  $\phi^n$  is given by

$$\phi^n = \phi_0^n + \phi_1^n : (\boldsymbol{\sigma}^0 + p^n \mathbf{I}) - \frac{\phi_0^n p^n}{\kappa}, \quad (55)$$

where  $\phi_0^n$  and  $\phi_1^n$  are the stress-free porosity and the first-order correction, respectively, and we assume both the factors  $p/\kappa'$  and  $\phi_1^n : \boldsymbol{\sigma}^0 / \phi_0$  to be small. The flow is governed by local mass transport

$$\frac{\partial}{\partial t} (\rho'^n \phi^n) = -\frac{\phi_0^n \rho_0}{\kappa' \tau} (p^n - p) \quad (56)$$

and global Darcy flow

$$\frac{\partial}{\partial t} \left( \sum_n \rho'^n \phi^n \right) = \nabla \cdot \left( \frac{\rho'}{\eta} \mathbf{K}^r \cdot \nabla p \right), \quad (57)$$

where  $\rho'^n$  is the density of the fluid within the  $n$ th crack,  $\kappa'$  is the bulk modulus of the fluid,  $\rho'$  is the average fluid density,  $p$  is the average (local) fluid pressure,  $\eta$  is the fluid viscosity,  $\mathbf{K}^r$  is the permeability tensor of the matrix and  $\tau$  is a relaxation parameter that characterizes the timescale of pressure equalization between neighbouring cracks. Using the relation between the fluid pressure and the density in the  $n$ th crack

$$\frac{\rho_0}{\rho'^n} - 1 = -\frac{p^n}{\kappa'}, \quad (58)$$

we derive the result

$$p^n = H_{ij}^n \sigma_{ij}^0 \quad (59)$$

where

$$H^n = \frac{\kappa'}{1 - i\omega\tau\gamma^n} \left[ i\omega\tau \frac{\phi_1^n}{\phi_0^n} - \sum_m \frac{\phi_1^m}{1 - i\omega\tau\gamma^m} \times \left( \sum_m \frac{\gamma^m \phi_0^m}{1 - i\omega\tau\gamma^m} + \frac{i\omega \hat{k}_p K_{pq}^r \hat{k}_q \kappa'}{v^2 \eta} \right)^{-1} \right], \quad (60)$$

$$\gamma^n = 1 + \frac{\kappa' \text{tr} \phi_1^n}{\phi_0^n}, \quad (61)$$

where  $v$  is a zeroth-order approximation to the wave speed and  $\text{tr}$  is the trace operator. Hence

$$e_{ij}^n = \left[ \bar{E}_{ijkl}^n s_{klmn}^0 + \left( \bar{E}_{ijrs}^n s_{klpp}^0 - \frac{\delta_{ij}}{3\kappa} \right) H_{mn}^n \right] \sigma_{mn}^0. \quad (62)$$

If we identify the right-hand side of eq. (62) with  $\hat{E}_{ijkl}^n s_{klmn}^0 \sigma_{mn}^0$ , this defines  $\hat{E}_{ijkl}^n$  as

$$\hat{E}_{ijkl}^n = \bar{E}_{ijkl}^n + \left( \bar{E}_{ijrs}^n s_{rspp}^0 - \frac{\delta_{ij}}{3\kappa} \right) H_{mn}^n c_{mnkl}^0. \quad (63)$$

We may then write

$$c_{ijkl}^1 = \sum_n s^n c_{ijpq}^+ \hat{E}_{mnpq}^n I_{mp}^n I_{nq}^n I_{rk}^n I_{sl}^n, \quad (64)$$

where

$$\hat{E}_{mnpq}^n = \hat{E}_{tuvx}^n I_{mt}^n I_{nu}^n I_{rv}^n I_{sx}^n = \bar{E}_{mnpq}^n + \frac{1}{3\kappa} (\bar{E}_{mnuu}^n - \delta_{mn}) H_{vx}^n c_{vxrs}^0, \quad (65)$$

$$H_{vx}^n = H_{ijvi}^n I_{xj}^n \quad (66)$$

and we have made use of the relation

$$\bar{E}_{mntu}^n s_{tupp}^0 = \frac{1}{3\kappa} \bar{E}_{mnuu}^n. \quad (67)$$

It remains to calculate  $\phi_1^n$ . As with Hudson *et al.* (1996) we approximate  $\phi_1^n$  using the result for a single crack. The relative increase in volume of an empty crack under the imposed stress  $\sigma^0$  is

$$\frac{\phi^n - \phi_0^n}{\phi_0^n} = \frac{\phi_1^n : \sigma^0}{\phi_0^n} = \frac{1}{V} \int_V e_{ii}^n dV = \bar{E}_{iikl}^n s_{klpq}^0 \sigma_{pq}^0, \quad (68)$$

so that

$$(\phi_1^n)_{pq} = \phi_0^n \bar{E}_{iikl}^n s_{klpq}^0 = \phi_0^n \bar{E}_{iirs}^n I_{rk}^n I_{sl}^n s_{klpq}^0 \quad (69)$$

and hence

$$H_{vx}^n c_{vxrs}^0 = \frac{\kappa'}{1 - i\omega\tau\gamma^n} \left[ i\omega\tau \bar{E}_{pprs}^n - I_{rk}^n I_{sl}^n \sum_m \frac{\phi_0^m \bar{E}_{pprtu}^m I_{tk}^m I_{ul}^m}{1 - i\omega\tau\gamma^m} \times \left( \sum_m \frac{\gamma^m \phi_0^m}{1 - i\omega\tau\gamma^m} + \frac{i\omega \hat{k}_p K_{pq}^r \hat{k}_q \kappa'}{v^2 \eta} \right)^{-1} \right] \quad (70)$$

and

$$\gamma^n = 1 + \frac{\kappa'}{3\kappa} \bar{E}_{iijj}^n. \quad (71)$$

### 5.1 The aligned thin-crack limit

If we make the assumption that the cracks are all aligned and of identical dimension, then we may write

$$c_{ijkl}^1 = s c_{ijpq}^+ \hat{E}_{pqkl}, \quad (72)$$

where

$$\hat{E}_{pqkl} = \bar{E}_{pqkl} + \frac{\kappa'}{3\kappa} (\bar{E}_{pquu} - \delta_{pq}) \chi \bar{E}_{vvkl}, \quad (73)$$

$$\chi = \frac{1}{1 - i\omega\tau\gamma} \left[ i\omega\tau - \frac{1}{\gamma + i\omega\tau K_2 (1 - i\omega\tau\gamma)} \right] \quad (74)$$

and

$$K_2 = \frac{\kappa' \hat{k}_p K_{pq}^r \hat{k}_q}{s v^2 \tau \eta}, \quad (75)$$

after Tod (2002).

In the limit  $\alpha \rightarrow 0$ , a number of components of  $\hat{E}$  vanish and eq. (72) reduces to the same limit as the fluid-filled isolated case does, in which  $c^1$  is given by eq. (28) and  $U_{33} = 0$ .

### 5.2 Results with fluid flow

Taking the same properties for the wave speeds and densities of the matrix and liquid infill and of the crack dimensions and number density as used previously, we assume an isotropic permeability such that  $K_{pq}^r = K^r \delta_{pq}$ , hence

$$K_2 = \frac{\kappa' K^r}{s v^2 \tau \eta} \quad (76)$$

and we now look at the sensitivity of the wave speeds to frequency  $f = \omega/2\pi$  with the offset and azimuth fixed at  $\theta = 30^\circ$  and  $\phi = 30^\circ$ .

Taking  $v = v_s$ ,  $K^r = 10^{-11} \text{ m}^2$ ,  $\eta = 10^{-4} \text{ Pa s}$  and  $\tau = 10^{-4} \text{ s}$ —at the upper end of the theoretical estimates by Hudson *et al.* (1996) and O'Connell & Budiansky (1977)—Fig. 4 shows the variation in wave speeds with  $f$ .

Now, the frequency dependence is contained entirely within the parameter  $\chi$  (eq. 74). In particular, the parameters  $\tau$ ,  $\gamma$  and  $K_2$  determine the sensitivity of  $\chi$  to  $f$ . For given matrix and fluid wave speeds and densities and given crack parameters, the sensitivity of  $\chi$  to  $f$  is controlled by  $\tau$  and the ratio  $K^r/\eta$ . A decrease in the ratio  $K^r/\eta$  by two orders of magnitude will increase the lowest frequency at which the wave speeds are significantly different from their zero-frequency limiting values by an order of magnitude, while an increase in  $K^r/\eta$  will have the opposite effect. The role of  $\tau$  is a little more complex, Fig. 5 is the same as Fig. 4, but with  $\tau = 10^{-6}$ , at the lower end of the theoretical estimates mentioned.

This modelling has assumed that fluid flow is the sole mechanism by which a frequency dependence may arise in the observed velocities when, in fact, there is an additional mechanism that may give rise to this phenomena: scattering. Certainly, for the larger frequencies shown in Figs 4(a) and (b) the wavenumber becomes comparable with the crack dimension and the effects of scattering must be included within a more complete theory, while at the larger frequencies shown in Figs 5(a) and (b) scattering is likely to dominate any observed effects of frequency dependence.

Figs 4(a) and (b) tell us that provided the fluid is sufficiently viscous and/or the matrix is sufficiently permeable and the relaxation time is large enough, the effect of the fluid flow mechanism is apparent within the seismic frequency band, where the compressional

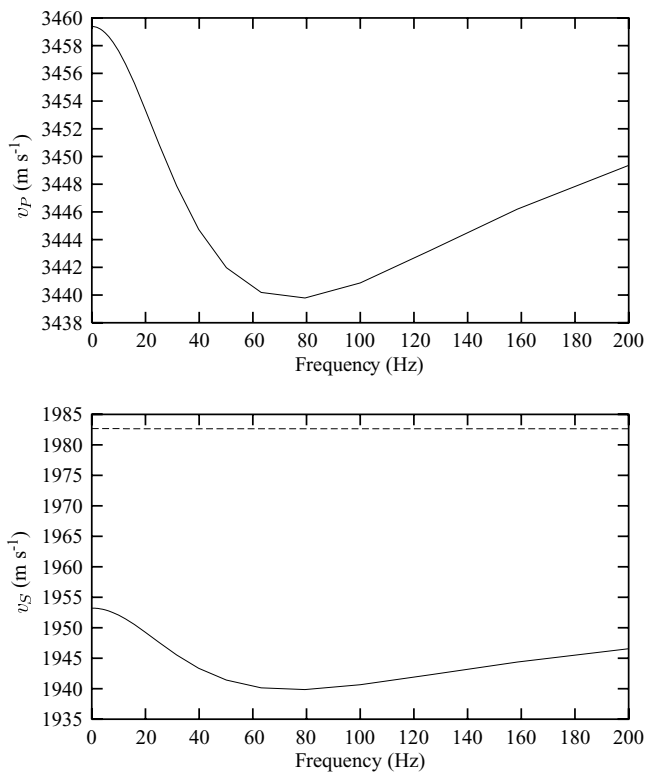


**Figure 4.** (a) The variation in compressional wave speed with frequency at  $\tau = 10^{-4}$  s and  $K'/\eta = 10^{-7}$  m<sup>2</sup> Pa<sup>-1</sup> s<sup>-1</sup>. (b) As in (a), but for shear wave speeds. The solid line corresponds to the quasi-SV wave and the dashed line to the quasi-SH wave.

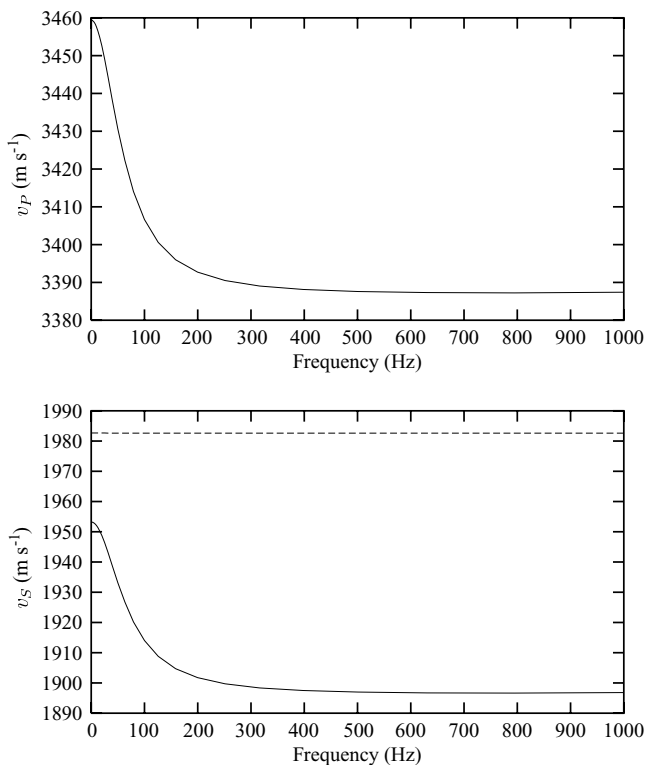


**Figure 5.** (a) As Fig. 4(a), but with  $\tau = 10^{-6}$  s. (b) As in (a), but for shear wave speeds. The solid line corresponds to the quasi-SV wave and the dashed line to the quasi-SH wave.

wave and one of the shear waves show small but non-negligible variations with frequency, whereas this frequency dependence will have all but vanished at logging and ultrasonic frequencies. While not frequency independent, the second shear wave has a negligible frequency dependence. Figs 5(a) and (b) suggest that for lower values of the relaxation parameter  $\tau$  the wave speeds are appreciably frequency dependent at seismic and at higher frequencies where the wave speeds rise steadily towards their high-frequency limit (not shown).

**6 CONCLUSIONS**

The commonly used Hudson theory (Hudson 1980, 1981) that was extended to include elliptical cracks of arbitrary dimensions (Hudson 1994) has been studied in detail to look at the effects of changing crack shape on the wave speeds of the effective medium, with particular application to bed-limited cracks, i.e. cracks where the vertical dimension is restricted because of the structure of the matrix material, but where the length is unconfined and the width is non-zero. As a limiting value of the general result valid for arbitrary shape, simple expressions are derived for the elastic stiffnesses in the case of flat elliptical cracks that take the same form as the original expressions given by Hudson (1981) and that reduce to those original expressions in the further limit in which the two parameters controlling the shape of the ellipse are identical.

In addition to this, the theory has been extended to incorporate a model of fluid flow that is dominated by the flow from one crack to another (Hudson *et al.* 1996; Tod 2001) and is valid at all frequencies such that the wavenumber remains less than the largest crack dimension. The simplest case, in which the cracks are taken to be all aligned and of identical dimension, is studied in some detail.

We are able to model the offset and azimuthal dependence of the material properties and the effects of changing crack dimensions with application to the inversion of seismic data for material properties. Furthermore, interpreting the frequency variation of the material properties has application to improving the understanding of the relation between wavespeeds measured in well logs and those interpreted from seismic data.

Tod & Liu (2002) use the theory to model the observed frequency dependence within both exploration and earthquake data in terms of fluid effects, while the development of a combined scattering/fluid-flow theory remains the subject of future work.

**ACKNOWLEDGMENTS**

The author would like to thank John A. Hudson at DAMTP, University of Cambridge and Enru Liu at the British Geological Survey for support and encouragement, and the anonymous reviewers for their helpful comments. The work was sponsored by the Natural Environment Research Council through project GST022305, as part of the thematic programme *Understanding the micro-to-macro behaviour of rock fluid systems* ( $\mu$ 2M) and is published with the approval of the Executive Director of the British Geological Survey (NERC).

**REFERENCES**

Anderson, D.L., Minster, B. & Cole, D., 1974. The effect of oriented cracks on seismic velocities, *J. geophys. Res.*, **79**, 4011–4015.  
 Auriault, J.L. & Boutin, C., 1994. Deformable porous media with double porosity. III: Acoustics, *Transp. Por. Med.*, **14**, 143–162.

- Bai, T., Pollard, D.D. & Gross, M.R., 2000. Mechanical prediction of fracture aperture in layered rocks, *J. geophys. Res.*, **105**, 707–721.
- Biot, M.A., 1956. Theory of propagation of elastic waves in a fluid-saturated porous solid. I. Low-frequency range, *J. acoust. Soc. Am.*, **28**, 168–178.
- Borgos, H.G., Cowie, P.A. & Dawers, N.H., 2000. Practicalities of extrapolating one-dimensional fault and fracture size–frequency distributions to higher-dimensional samples, *J. geophys. Res.*, **105**, 28 377–28 391.
- Budiansky, B. & O’Connell, R.J., 1976. Elastic moduli of a cracked solid, *Int. J. Solids Struct.*, **12**, 81–97.
- Chapman, M., 2001. Modelling the wide-band laboratory response of rock samples to fluid and pressure changes, *PhD thesis*, University of Edinburgh.
- Chesnokov, E.M., Queen, J.H., Vichorev, A.A., Lynn, H.B., Hooper, J.M., Bayuk, I.O., Castagna, J.A. & Roy, B., 2001. Frequency dependent anisotropy, in *Exp. Abs., 71st Ann. Int. Mtg SEG*, San Antonio, TX.
- Eshelby, J.D., 1957. The determination of the elastic field of an ellipsoidal inclusion and related problems, *Proc. R. Soc. Lond., A.*, **241**, 376–396.
- Garbin, H.D. & Knopoff, L., 1973. The compressional modulus of a material permeated by a random distribution of circular cracks, *Q. appl. Math.*, **30**, 453–464.
- Garbin, H.D. & Knopoff, L., 1975. Elastic moduli of a medium with liquid-filled cracks, *Q. appl. Math.*, **33**, 301–303.
- Gassmann, F., 1951. Über die elastizität poröser medien, *Vier. Natur. Gesell. Zurich*, **96**, 1–23.
- Gradshteyn, I.S. & Ryzhik, I.M., 1980. *Tables of Integrals, Series, and Products*, 4th edn, Academic Press, New York.
- Hudson, J.A., 1980. Overall properties of a cracked solid, *Math. Proc. Camb. Phil. Soc.*, **88**, 371–384.
- Hudson, J.A., 1981. Wave speeds and attenuation of elastic waves in material containing cracks, *Geophys. J. R. astr. Soc.*, **64**, 133–150.
- Hudson, J.A., 1994. Overall properties of materials with inclusions or cavities, *Geophys. J. Int.* **117**, 555–561.
- Hudson, J.A., Liu, E. & Crampin, S., 1996. The mechanical properties of materials with interconnected cracks and pores, *Geophys. J. Int.* **124**, 105–112.
- Keller, J.B., 1964. Stochastic equations and wave propagation in random media, *Proc. Symp. appl. Math.*, **16**, 145–170.
- Kuster, G.T. & Toksöz, M.N., 1974. Velocity and attenuation of seismic waves in two-phase media: Part 1. Theoretical formulations, *Geophysics*, **39**, 587–606.
- Lore, J., Aydin, A. & Goodson, K., 2001. A deterministic methodology for prediction of fracture distribution in basaltic multiflows, *J. geophys. Res.*, **106**, 6447–6459.
- Mavko, G.M. & Jizba, D., 1991. Estimating the grain-scale fluid effects on velocity dispersion in rocks, *Geophysics*, **56**, 1940–1949.
- Mavko, G.M. & Nur, A., 1978. The effect of nonelliptical cracks on the compressibility of rocks, *J. geophys. Res.*, **83**, 4459–4468.
- Nishizawa, O., 1982. Seismic velocity anisotropy in a medium containing orientated cracks—transversely isotropic case, *J. Phys. Earth*, **30**, 331–347.
- O’Connell, R.J. & Budiansky, B., 1974. Seismic velocities in dry and saturated cracked solids, *J. geophys. Res.*, **79**, 5412–5426.
- O’Connell, R.J. & Budiansky, B., 1977. Viscoelastic properties of fluid-saturated cracked solids, *J. geophys. Res.*, **82**, 5719–5735.
- Rathore, J.S., Fjaer, E., Holt, R.M. & Renlie, L., 1995. *P*- and *S*-wave anisotropy of a synthetic sandstone with controlled crack geometry, *Geophys. Prospect.*, **43**, 711–728.
- Roy, B., Hooper, J., Queen, J., Bayuk, I., Kukharenko, Y. & Chesnokov, E., 2001. Prediction of frequency dependent velocity in porous reservoirs, in *Exp. Abs., 71st Ann. Int. Mtg SEG*, San Antonio, TX.
- Sayers, C.M., 1988. Inversion of ultrasonic wave velocity measurements to obtain the microcrack orientation distribution function in rocks, *Ultrasonics*, **26**, 73–77.
- Shapiro, S.A. & Hubral, P., 1996. Elastic waves in finely layered sediments: the equivalent medium and generalized O’Doherty–Anstey formulas, *Geophysics*, **61**, 1282–1300.
- Sothcott, J., McCann, C. & O’Hara, S.G., 2000. The influence of two different pore fluids on the acoustic properties of reservoir sandstones at sonic and ultrasonic frequencies, in *Exp. Abs., 70th Ann. Int. Mtg SEG*, Calgary, Canada.
- Spencer, J.W., 1981. Stress relaxation at low frequencies in fluid-saturated rocks: attenuation and modulus dispersion, *J. geophys. Res.*, **86**, 1803–1812.
- Thomsen, L., 1995. Elastic anisotropy due to aligned cracks in porous rock, *Geophys. Prospect.*, **43**, 805–829.
- Tod, S.R., 2001. The effects on seismic waves of interconnected nearly aligned cracks, *Geophys. J. Int.* **146**, 249–263.
- Tod, S.R., 2002. The effects of stress and fluid pressure on the anisotropy of interconnected cracks, *Geophys. J. Int.* **149**, 149–156.
- Tod, S.R. & Liu, E., 2002. Frequency-dependent anisotropy due to fluid flow in bed limited cracks, *Geophys. Res. Lett.*, **29**, 10.1029/2002GL015 369.
- Tsukrov, I., 2000. Elastic moduli of composites with rigid elliptical inclusions, *Int. J. Fract.*, **101**, L29–L34.
- Tsukrov, I. & Kachanov, M., 2000. Elastic moduli of an anisotropic material with elliptical holes of arbitrary orientational distribution, *Int. J. Solids Struct.*, **37**, 5919–5941.
- Tsukrov, I. & Novak, J., 2002. Effective elastic properties of solids with defects of irregular shapes, *Int. J. Solids Struct.*, **39**, 1539–1555.
- Walsh, J.B., 1965. The effect of cracks on the compressibility of rock, *J. geophys. Res.*, **70**, 381–389.
- Walsh, J.B. & Grosenbaugh, M.A., 1979. A new model for analyzing the effect of fractures on compressibility, *J. geophys. Res.*, **84**, 3532–3536.
- Winkler, K.W., 1985. Dispersion analysis of velocity and attenuation in Berea sandstone, *J. geophys. Res.*, **90**, 6793–6800.
- Ying, C.F. & Truell, R., 1956. Scattering of a plane longitudinal wave by a spherical obstacle in an isotropically elastic solid, *J. Appl. Phys.*, **27**, 1086–1097.

## APPENDIX A: DETERMINING $E$

The non-zero components of  $A^0$  (eq. 27) are

$$A_{1111}^0 = A_{2222}^0 = 1, \quad (A1)$$

$$A_{3311}^0 = A_{3322}^0 = \frac{1}{3(1-\nu)} \left[ (1+\nu) \frac{\kappa'}{\kappa} - (1-2\nu) \frac{\mu'}{\mu} - 3\nu \right], \quad (A2)$$

$$A_{3333}^0 = \frac{1}{3(1-\nu)} \left[ (1+\nu) \frac{\kappa'}{\kappa} + 2(1-2\nu) \frac{\mu'}{\mu} \right], \quad (A3)$$

$$A_{2323}^0 = A_{1313}^0 = \frac{1}{2} \frac{\mu'}{\mu}, \quad (A4)$$

$$A_{1212}^0 = \frac{1}{2} \quad (A5)$$

and those related to the above by the symmetries of eq. (26).

When  $\mu' = 0$ , the components of  $A^1$  that are required, are

$$A_{2323}^1 = \frac{aE}{2b(1-\nu)} [1 - \nu f(b/a)], \quad (A6)$$

$$A_{1313}^1 = \frac{aE}{2b(1-\nu)} \{1 + \nu[f(b/a) - 1]\} \quad (A7)$$

and those related to the above by the symmetries of eq. (26). When  $\kappa' = 0$  as well, we also need

$$A_{1133}^1 = \frac{1-2\nu}{2(1-\nu)} \frac{aE}{b} f(b/a), \tag{A8}$$

$$A_{2233}^1 = \frac{1-2\nu}{2(1-\nu)} \frac{aE}{b} [1 - f(b/a)], \tag{A9}$$

and

$$A_{3333}^1 = \frac{1-2\nu}{2(1-\nu)} \frac{aE}{b}. \tag{A10}$$

The components of  $\alpha E$  are related to those of  $A^0$  and  $A^1$  by

$$\alpha E_{2323} = \frac{1}{4A_{2323}^1} + \mathcal{O}(\alpha), \tag{A11}$$

$$\alpha E_{1313} = \frac{1}{4A_{1313}^1} + \mathcal{O}(\alpha) \tag{A12}$$

and those related to the above by the symmetries of eq. (26). If additionally  $\kappa' = 0$  then

$$\alpha E_{3311} = \alpha E_{3322} = \frac{-A_{3311}^0}{A_{3333}^1 - A_{3322}^0 A_{2233}^1 - A_{3311}^0 A_{1133}^1} + \mathcal{O}(\alpha), \tag{A13}$$

and

$$\alpha E_{3333} = \frac{1}{A_{3333}^1 - A_{3322}^0 A_{2233}^1 - A_{3311}^0 A_{1133}^1} + \mathcal{O}(\alpha), \tag{A14}$$

otherwise they are all  $\mathcal{O}(\alpha)$ .

With  $\mu' \neq 0$  and  $\kappa' \neq 0$  but  $\mu'/\mu$  and  $\kappa'/\kappa$  small, such that we may keep terms of the order  $\alpha\mu/\mu'$  and  $\alpha\kappa/\kappa'$  we may expand  $E$  to obtain

$$\begin{aligned} \alpha E_{3311} &= \alpha E_{3322} \\ &= \frac{-A_{3311}^0}{A_{3333}^0/\alpha + A_{3333}^1 - A_{3322}^0 A_{2233}^1 - A_{3311}^0 A_{1133}^1}, \end{aligned} \tag{A15}$$

$$\alpha E_{3333} = \frac{1}{A_{3333}^0/\alpha + A_{3333}^1 - A_{3322}^0 A_{2233}^1 - A_{3311}^0 A_{1133}^1}, \tag{A16}$$

$$\alpha E_{2323} = \frac{1}{4(A_{2323}^0/\alpha + A_{2323}^1)}, \tag{A17}$$

$$\alpha E_{1313} = \frac{1}{4(A_{1313}^0/\alpha + A_{1313}^1)} \tag{A18}$$

and those related to the above by the symmetries of eq. (26).